ELSEVIER

Materials Science and Engineering A 447 (2007) 324–331

MATERIALS SCIENCE & ENGINEERING A

www.elsevier.com/locate/msea

Stability of Cu–Zn phases under low energy ball milling

J. Andrade-Gamboa [a], F.C. Gennari [b], P. Arneodo Larochette [b], C. Neyertz [a], M. Ahlers [a], J.L. Pelegrina [b,*]

[a] *Centro Atómico Bariloche, Av. E. Bustillo 9500, R8402AGP San Carlos de Bariloche, Argentina*
[b] *Centro Atómico Bariloche and CONICET, Av. E. Bustillo 9500, R8402AGP San Carlos de Bariloche, Argentina*

Received 19 July 2006; received in revised form 3 October 2006; accepted 26 October 2006

Abstract

Low energy ball milling of equiatomic Cu–Zn has been performed. The β phase alloy has shown to be stable under this mechanical processing, with no signs of the appearance of other crystalline or amorphous phases. It was determined that the B2 order is retained. The evolution of the phases during mechanical alloying of equiatomic amounts of the pure elements was also investigated. It was found that the speed of the process depends on the milling configuration. It was also determined that the powder temperature on milling does not exceed 373 K. Low temperature thermal treatments allowed to extend down to 373 K the β phase field range in the phase diagram. This novel result could be obtained due to the unique properties of ball milling, which permits to reach phases in the phase diagram following low temperature paths.
© 2006 Elsevier B.V. All rights reserved.

Keywords: Copper alloys; Lattice defects; Mechanical alloying; Mechanical milling; Phase stability

1. Introduction

The Cu–Zn system is rich in equilibrium and nonequilibrium phases. The assessed phase diagram [1], shown in Fig. 1, indicates the presence of two terminal solid solutions: α (or Cu) with an fcc structure and η (or Zn) which is hcp. The intermetallic phases and their structures are β (bcc), β′ (ordered bcc), γ (complex cubic), δ and ε which are hexagonal. The β′ phase has a CsCl structure (B2) which has been found to transform to two metastable phases of Cu–Zn. One of them is called 9R, an orthorhombic nine layer stacking sequence of close packed planes [2]. This transition occurs on cooling β′ or by applying stresses, and is of the martensitic type. The other metastable phase appears at higher temperatures when the intermetallic is dezincified. The resulting structure is hexagonal and was described as a four layer stacking of close packed planes [3].

The solid state processing of materials by mechanical alloying and/or milling has become of widespread interest due to its capabilities to produce equilibrium and nonequilibrium phases as well [4]. The former technique involves material transfer (alloying), but in both cases the final phase is homogeneous in composition. Mechanical alloying is rationalized as a random sequence of plastic deformation, cold welding and fracture. In order to understand the mechanism of this process, different interpretations of mechanical deformation-induced nanocrystal formation, amorphization and/or crystallization of amorphous phases have been proposed. One mechanism suggests that during milling, the local effective temperature can rise in the severely deformed regions as a result of high energetic collisions, allowing the welding process or the amorphous formation [5]. Other mechanism proposes that heavy deformation is introduced into the particles through dislocations, stacking faults, vacancies and increased number of grain boundaries. The presence of these defects and the nanoscale microstructural features enhance the diffusion of the elements. In this case, the jumps could be favored by high local temperatures, but the mechanical alloying process should happen nominally at room temperature [4].

Several microstructural changes were shown to take place during milling. Characterization of these changes involves determination of crystallite sizes, internal strains and defects, such as dislocations and stacking faults. The crystallite sizes are often extracted from X-ray diffraction peak broadening. However, since strain and faults also affect peak profiles, a suitable analysis is necessary to separate each contribution. In general, mechanical treatments introduce strain and stacking faults, and their

* Corresponding author. Fax: +54 2944 445299.
E-mail address: jlp201@cab.cnea.gov.ar (J.L. Pelegrina).

0921-5093/$ – see front matter © 2006 Elsevier B.V. All rights reserved.
doi:10.1016/j.msea.2006.10.134

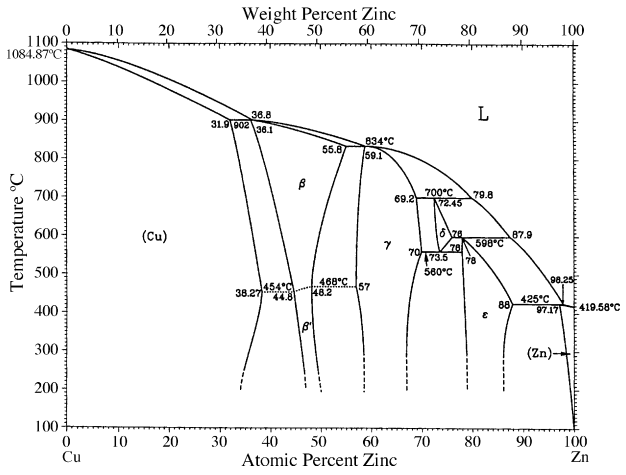

Fig. 1. Cu–Zn phase diagram after Ref. [1].

evolutions with milling time depend on sample structure and milling conditions [4].

The Cu–Zn system has been extensively studied by *high energy* ball milling [6–8]. The formation of the β phase from the elements has been given as a proof of the real alloying capabilities of the technique [7]. It has been found that the zinc rich phases form first [6,8]. This was attributed to the difference in diffusivity of the elements, which becomes more evident at the first stages, when the crystallite size is still large and has not been reduced to the nanometer scale by milling. It has also been found that the system evolves to β by passing through a sequence of intermediate phases, which are only those pertaining to the low temperature part of the equilibrium phase diagram [6,8].

To the authors knowledge, the Cu–Zn system has not been studied by *low energy* ball milling. This is surprising, since it is known that soft milling conditions seem to favor the formation of metastable phases [4]. In the present work, the stability under low energy mechanical milling of an equiatomic β phase alloy (prepared by melting the elements) has been studied. The evolution of the phases from the pure elements to the β phase under different milling configurations will be also reported. In both cases, the contribution of strains, stacking faults and crystallite sizes on the XRD peak broadening was analyzed as a function of milling time.

2. Experimental

A Cu–50 at%Zn alloy of 100 g was prepared from pure metals (99.99%) in sealed quartz tubes, within an Ar atmosphere, using a resistance furnace. The resulting button was cut and its homogeneity was verified by wavelength dispersive spectroscopy in a scanning electron microscope. Afterwards, it was filed to obtain the powder to be milled, which was thermally treated at 373 K for 24 h to reduce internal stresses. The latter was performed inside a quartz capsule in an Ar atmosphere, and the efficiency of the treatment was verified by the reduction of the width of the X-ray diffraction peaks.

Pure (99.99%) Cu and Zn were also filed to obtain the starting powders for mechanical alloying. They were not heat treated and the used quantities were in accordance to an equiatomic composition.

The powder processing was carried out in an Uni-Ball-Mill II equipment manufactured by Australian Scientific Instruments (Canberra, Australia). It has a rotating cylindrical hardened steel cell of around 200 mm diameter and 29 mm height. Seven bearing balls of 25.4 mm diameter (67 g each) were used. The trajectory of the balls can be modified by an external magnetic field, produced by a V-shaped permanent magnet. A comparison of the alloying process was done for two different positions of the magnet, which give two milling configurations, here called low and high. A scheme of these two milling configurations is presented in Fig. 2. The cell rotates anticlockwise and the dotted lines indicate the widest trajectory of the balls [9]. These paths have been directly observed by video recordings, replacing the

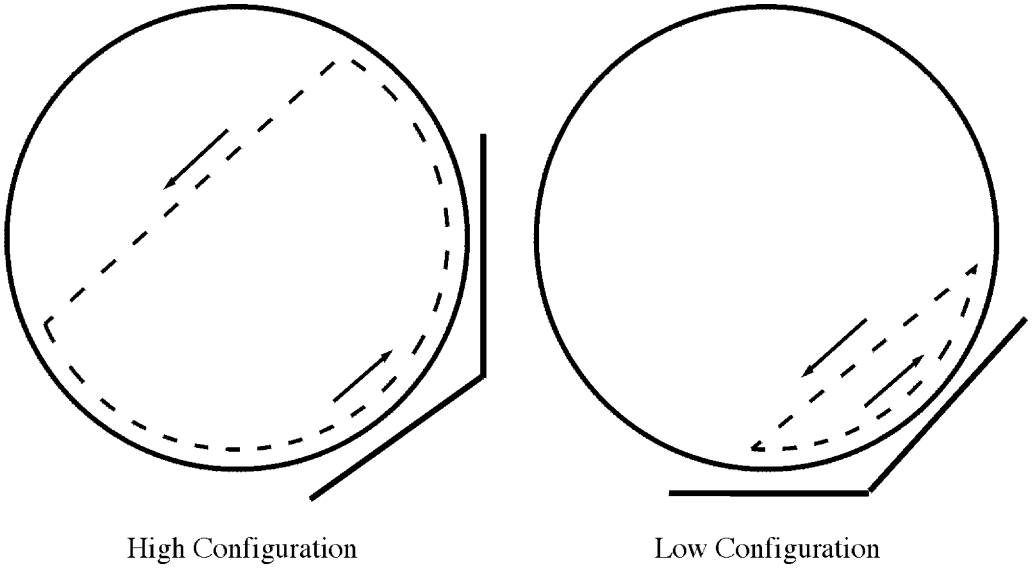

Fig. 2. Schematic diagram of the cylindrical milling chamber, view from the rotation axis. The V-shaped permanent magnet is also shown. The dotted lines indicate the ball trajectories.

steel cover of the chamber by a transparent one. It has to be noted that the balls also move according to the shearing mode [9]. The powder charge was of 10 g, implying a powder-to-ball ratio of nearly 47. An Ar atmosphere with an overpressure of around 0.5 MPa and a rotation speed of 177 rpm were used. At each sampling, 0.2 g of powder was removed. The powder was scrapped from the walls when agglomeration and sticking effects were observed. Afterwards, the Ar atmosphere was established again.

X-ray powder diffraction patterns (diffractograms) were taken with a Philips PW1710/01 diffractometer using Cu Kα radiation and a graphite monocromator. The scans were recorded between 20° and 90° using a step of 0.02° and a counting time of 1 s. The Rietveld refinement method [10] was used to confirm the presence of the different structures from each diffractogram.

The thermal analysis was carried out using a TA 2910 DSC calorimeter, working at 5 K/min scanning rates and with an Ar flow of 120 ml/min. The sample consisted of around 60 mg of powder in an Al pan and an empty pan was used as the reference.

Samples for transmission electron microscopy were obtained by dispersing a little amount of the powder in ethanol and putting a drop of the mixture in a carbon grid. The observations were made in a Philips CM200UT transmission electron microscope (TEM) operating at 200 kV.

3. Results

3.1. Mechanical milling of the β phase alloy

For the study of the effect of milling on the β phase alloy, the high configuration (see Section 2) was applied. Fig. 3a shows the diffractograms of the alloy milled for 320 h (solid line) and of the same sample after a short heating treatment (see Section 3.3) at 573 K (dotted line). For both cases neither a sign of decomposition nor of transformation was found. For the intermediate milling times similar diffractograms were obtained, the only change being the width of the reflections. For each peak the full width at half maximum (corrected for instrumental broadening using a silicon standard) was calculated as a function of milling time. From these values, shown in Fig. 3b, it is concluded that the peaks widen up to 40 h of milling and then remain unchanged.

A dark field transmission electron micrograph of the alloy milled for 320 h is shown in Fig. 4a, and the corresponding diffraction pattern in Fig. 4b. It can be seen that a crystallite size of around 5 nm was obtained. The electron diffraction pattern indicates that no amorphous phase is present. It can be consistently indexed as that corresponding to the B2 ordered phase. This indicates that the alloy as well as the order are stable under the action of low energy mechanical milling.

3.2. Mechanical alloying of the pure elements

Fig. 5 shows the diffractograms of the mixture of the pure elements at shorter milling times and for both configurations. Only the main part of the diffractograms is shown, for a better resolution of the peaks and its corresponding phases. It can be seen that after 0.5 h of alloying, the phases present are α, ε and η, independent of the milling configuration. For increasing times, there is a speed up of the phase evolution for the low configuration. At 1.5 h the amount of ε phase, best observed from the peak at 42°, passes through a maximum and the γ phase already appears, whereas for the high configuration there is no evidence of such features. For this latter configuration, the ε maximum occurs at around 2 h of milling, but with a reduced relative diffraction intensity, indicating a lower amount of this phase, and γ appears only after 2.5 h. In agreement with the increased rate of phase formation for the low configuration, the η phase completely disappeared after processing for 2.5 h, while it remains up to 6 h for the high configuration.

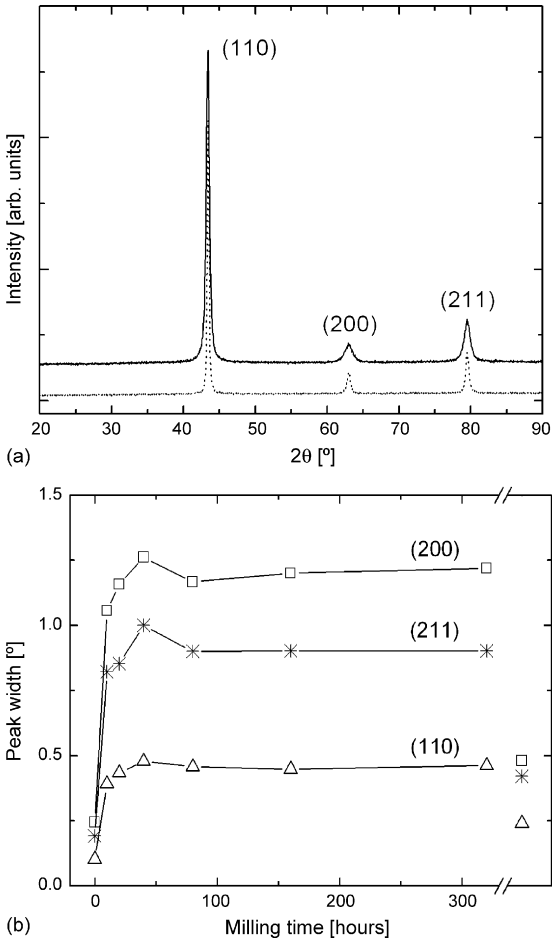

Fig. 3. (a) XRD patterns of the β phase alloy after milling for 320 h (solid line) and the same sample after being heated up to 573 K (dotted line). The patterns were shifted for clarity. (b) β Phase peak width as a function of the milling time. The isolated points to the right of the figure correspond to the dotted line in (a) (i.e. no additional milling time). The error bars define an interval of the same height as the symbols.

For higher milling times the final stage for both configurations is solely β phase which is fully formed after 80 and 20 h for the high and low configuration, respectively. Fig. 6 shows the diffractograms corresponding to 8, 10 and 20 h of milling at the low configuration. The peaks of the β phase overlap those of γ and therefore the presence of the former can be visually confirmed only when the latter disappears. It is very important to note that in no case the presence of oxides was detected.

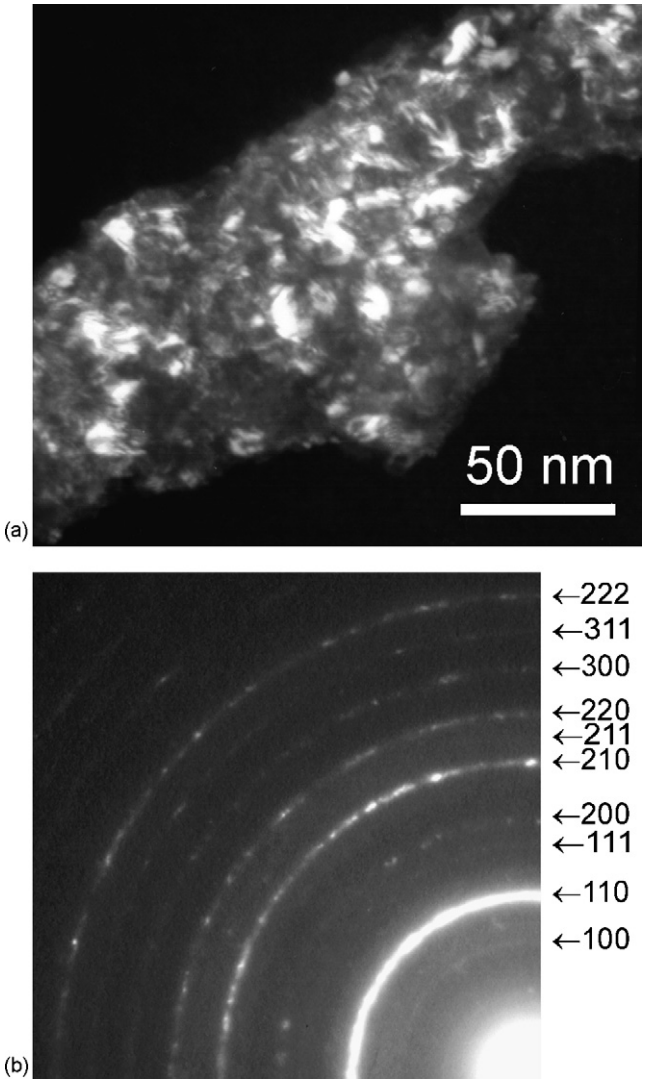

Fig. 4. (a) Dark field micrograph of the β phase alloy after milling for 320 h. (b) Selected area diffraction pattern of the same zone.

3.3. Calorimetry of the powders

To analyze the thermal stability of the milled samples (both the β alloy and the elemental powders) different calorimetric runs were performed up to 573 K. Fig. 7 shows the exothermal peaks obtained after heating the milled samples under the high configuration. Only the first part of the scans is shown, where the main evolution occurs, while at higher temperatures they still do not return to the base line and do not show further peaks. The first letter that labels each curve designates if it arose from the pure elements (E) or from the alloy (A). The numbers that appear next indicate the milling time in hours. From the calorimetric curves it can be established that the ball-milled elements present the maximum value of released heat, which diminishes as a function of the milling time. For curve E3, i.e. after 3 h of mechanical alloying the elements, the released heat is around 3 kJ/mol. It has to be taken into account that between 3 and 10 h, the sample is composed of a mixture of phases. In these cases, the measured heat arises from the elimination of stresses, crystallite growth and from the possible phase transformations, as it was determined from XRD (not shown). It is not possible to estimate the contribution of each process. Mechanical alloying of the pure elements for 80 h produced a powder of solely β phase, whose behavior on heating is depicted by E80. The estimated released heat is twice that obtained from the milled β phase (A80).

The most striking feature of Fig. 7 is that the thermal evolution of the material begins to be detectable at temperatures below 370 K. It is in agreement with the known evidence that diffusion in β Cu based alloys is detectable at room temperature [2]. Therefore, it was found of interest to analyze the phase evolution, of a powder obtained from the pure elements by milling during 6 h, when heated up to 373 K. Fig. 8a shows the as-milled sample consisting of a mixture of α, γ and ε phases. After annealing at 373 K for 1 h, the amount of β increased at the expense of the other phases (Fig. 8b). For comparison, the β phase diffractogram is shown in Fig. 8c. The amount of β phase which results from the Rietveld refinement of Fig. 8b is of the order of 40% in weight of the sample.

4. Discussion

4.1. Phase evolution during the milling of the mixture of pure elements

The low energy mechanical alloying of an equiatomic mixture of Cu and Zn atoms resulted in the formation of a pure β phase alloy. The mixture passed previously through a sequence of the low temperature equilibrium phases with higher Zn content, as reported in the literature for the high energy processing [6,8]. For each milling configuration the sequence of phase formation was the same. It was necessary to increase the processing times when the high configuration was used, in order to produce the appearance of the phases. This latter behavior can be rationalized by analyzing the terms that contribute to the specific milling dose D_m [11] for both configurations. This parameter is given by

$$D_m = \frac{NEt}{m_P} \quad (1)$$

where N is the impact frequency, E the impact energy, t the processing time and m_P is the mass of the powder batch. Therefore, as it is known that the reaction yield is an invariant quantity of each system [11], the speed of processing has to be related with the specific milling dose per unit time. So, mainly the product NE, that is the milling intensity, has to be analyzed because the powder mass is nearly the same in all trials. This will done next.

The balls in the milling chamber follow complex paths. Therefore, as a first approximation, the energy of the impact has to be defined as a mean value, estimated from a representative trajectory. The same happens with the impact frequency, because the process resembles more a chaotic than an ordered fall of the balls. The last feature that has to be taken into account is that the cell rotation gets the powder to be in the lower right quadrant. So, N and E had to be analyzed in either case for trajectories of the type shown at the right of Fig. 2. Wider paths,

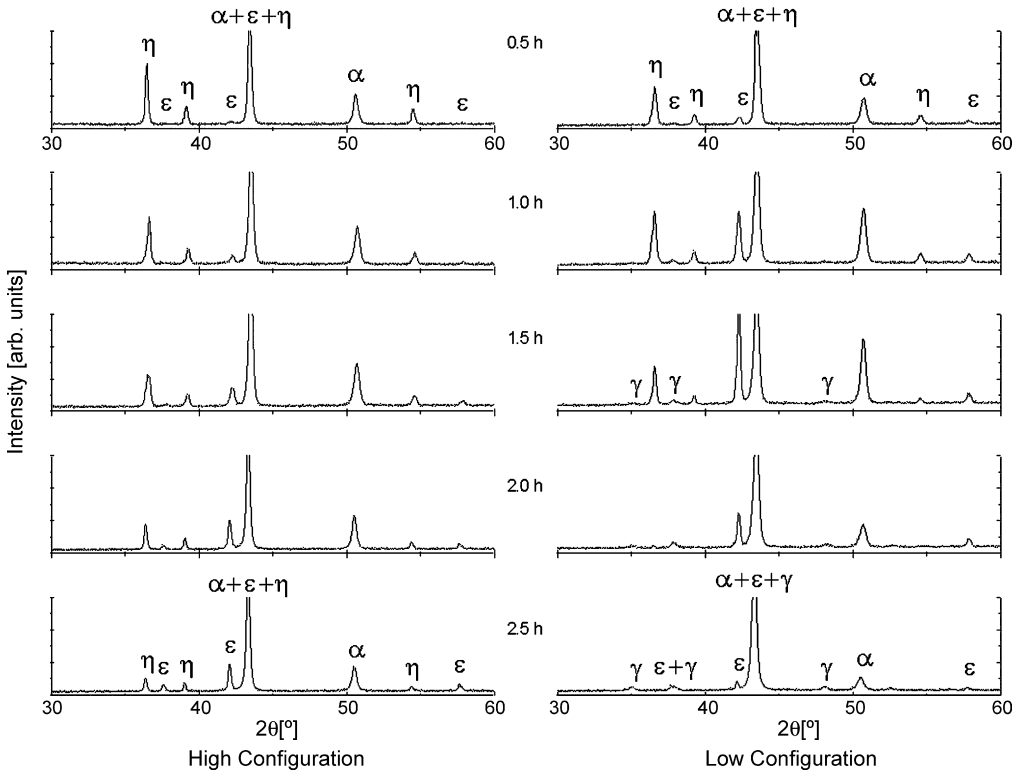

Fig. 5. XRD patterns of the first stages of mechanical alloying of the pure elements, for the two milling configurations. The intensity of the maximum peak exceeds the ordinate scale.

as those occurring for the high configuration, involve a lower amount of powder and were discarded. A mean impact energy of around 70 mJ/hit was calculated for the observed trajectory. The mean number of impacts in a given period of time was determined from video recordings. The impact frequency for the low configuration is a factor between two and three times greater than that for the high one. The energy received by the shearing action of the balls was judged to be negligible. It results that the milling intensity in the high configuration is less than half that in the low one, consistent with the slower evolution of the material when milled in the former configuration.

The previous estimate was appropriate for a rough evaluation of the milling intensity, but should not be used to calculate the

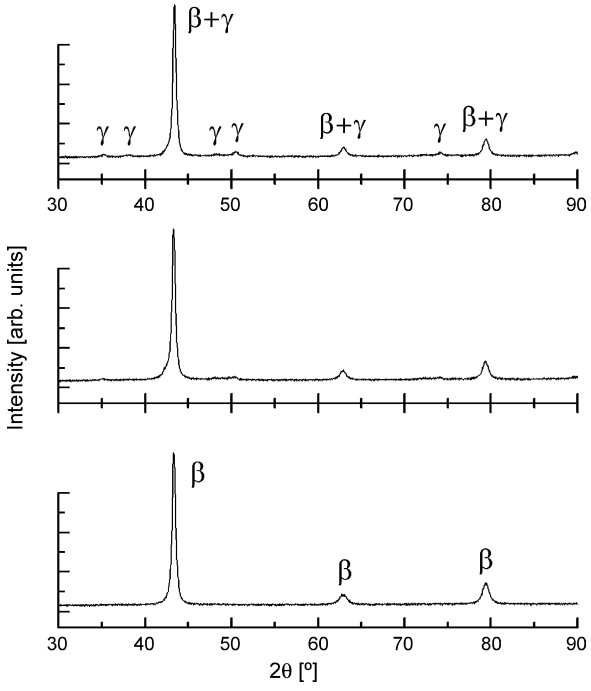

Fig. 6. XRD patterns of the final stages of mechanical alloying. They correspond to 8, 10 and 20 h (from top to bottom) for the low milling configuration.

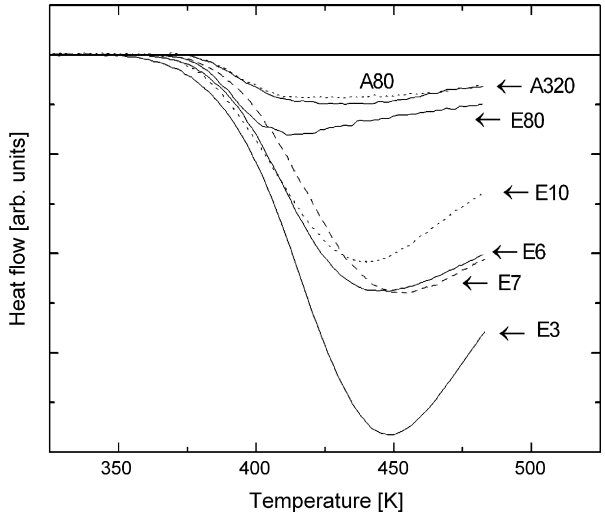

Fig. 7. DSC scan of the ball-milled alloy (indicated by an initial A) and of the elements (E) using the high configuration. The numbers that follow the previous letter correspond to the milling time in hours. The horizontal reference base line is indicated. The peaks are exothermic.

Table 1
Apparent crystallite sizes (D) and strains (ε) corresponding to specific diffraction peaks, for the different stages in the process of milling the β phase alloy

Stage	Peak					
	1 1 0		2 0 0		2 1 1	
	D [nm]	ε [%]	D [nm]	ε [%]	D [nm]	ε [%]
Powder from alloy in high configuration						
(1) As filed	53	0.39	19	0.64	33	0.35
(2) Annealed at 373 K during 24 h	250	0.16	90	0.21	140	0.12
(3) Milled for 10 h	44	0.45	17	0.71	27	0.30
(4) Milled for 160 h	38	0.51	15	0.81	23	0.38
(5) Milled for 320 h	38	0.52	15	0.83	24	0.37
(6) 320 h, heated up to 573 K	130	0.22	53	0.30	74	0.19
Powder from pure elements						
(7) 80 h in high configuration	33	0.62	14	0.93	22	0.51
(8) 20 h in low configuration	49	0.45	22	0.61	30	0.39

The last two rows correspond to the results for the long time alloyed pure elements in the high and low milling configurations, respectively.

specific milling dose. The before mentioned chaotic trajectories of the balls are in fact consistent with a distribution of milling intensities, which appears extremely difficult to be measured in this system with seven balls.

4.2. Microstructural changes of the β phase during milling

It was shown that the X-ray diffraction peaks of the milled β phase broadened for processing times up to 40 h (Fig. 3b). To detect from the width of the peaks the average size of the diffracting domains and the strain contribution, the Williamson–Hall method could not be applied, because a high anisotropy was found. Instead, a single line analysis was performed [12], from which size and strain contributions are derived, respectively, from the Lorentz and Gauss components of the peak profiles. Table 1 shows the results corresponding to the β phase alloy (milled only at the high configuration) and for the β phase formed from the pure elements for both milling configurations. From Table 1 it can be seen that for each sample, the crystallite size values obtained from each diffraction peak are different. This known effect, which is not always reported, is due to the presence of deformation and twin stacking faults on the {2 1 1} planes of the bcc structure [13]. The size contribution obtained from the analysis of the peak profiles is in fact an apparent crystallite size. The contribution of the stacking faults can be accounted by means of a fictitious crystallite size, D_F, as follows: Let D(h k l) be the apparent domain size obtained from each (h k l) reflection, then, it can be demonstrated [13] that

$$\frac{1}{D(\text{h k l})} = \frac{1}{D_I} + \frac{1}{D_F(\text{h k l})} \tag{2}$$

being D_I the real crystallite size (isotropous). The fictitious size depends on the specific diffraction peak and can be expressed as

$$\frac{1}{D_F(\text{h k l})} = (1.5\ \alpha + \beta)\frac{C(\text{h k l})}{a} \tag{3}$$

where $(1.5\alpha+\beta)$ is the faulting probability[1] and a is the lattice parameter. The constants C(h k l) take the values $\sqrt{2}/3$, $4/3$ and $2/\sqrt{6}$ for the 1 1 0, 2 0 0 and 2 1 1 peaks, respectively [13]. It can be seen from Eq. (2) that when the real crystallite size is big compared with D_F, the only contribution to the peak broadening arises from the stacking faults. In the general case, it is possible to calculate D_I and D_F from the data, and deduce the faulting probability from Eq. (3). These values are shown in Table 2. The crystallite size of the as filed material and of the annealed one as well were too big and could not be determined. It can be seen that the annealing at 373 K effectively reduced the faulting probability and the internal strains as well. On milling, the crystallite size decreased, within experimental scatter, and the strain and faulting probability increased until the steady state was reached. These results indicate that not only the width of the X-ray diffraction peak remain unchanged after 40 h of processing, but also the different contributions to the peak. This is confirmed by the measured negligible difference of the

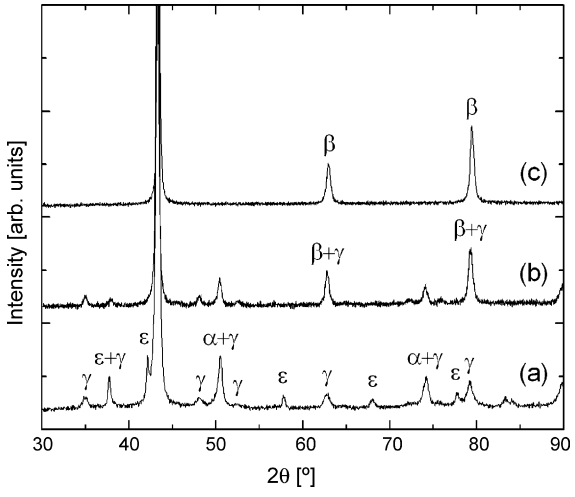

Fig. 8. (a) XRD pattern after milling for 6 h at the high configuration, (b) same as in (a) plus annealing at 373 K during 1 h and (c) XRD pattern of pure β phase. The patterns were shifted for clarity.

[1] The α and β faulting probability parameters should not be confused with the phases in the Cu–Zn system.

Table 2
Isotropic or real crystallite sizes (D_I) and faulting probabilities ($1.5\,\alpha + \beta$) for the milling stages of Table 1

Stage	D_I [nm]	$1.5\,\alpha + \beta$	σ(1 1 0) [MPa]	σ(2 0 0) [MPa]	σ(2 1 1) [MPa]
Powder from alloy in high configuration					
(1) As filed	–	0.0115	340	220	310
(2) Annealed at 373 K during 24 h	–	0.0025	140	70	110
(3) Milled for 10 h	340	0.0124	400	250	260
(4) Milled for 160 h	210	0.0138	450	280	340
(5) Milled for 320 h	260	0.0139	460	290	330
(6) 320 h, heated up to 573 K	400	0.0037	190	100	170
Powder from pure elements					
(7) 80 h in high configuration	140	0.0142	550	320	450
(8) 20 h in low configuration	120	0.0085	400	210	340

The stresses for each diffraction peak [σ(h k l)] were obtained from the strains in Table 1.

curves A80 and A320 in Fig. 7. In this steady state, at least after 80 h of milling, any deformation produced by the process should be simultaneously annealed out. The steady state values reached in Fig. 3b were altered by heating to 573 K in the DSC followed by immediate cooling. In spite of a higher annealing temperature, the reduction of internal strains and stacking faults, and the increase of the domain size were less pronounced than in the initial treatment at 373 K.

From Tables 1 and 2, it can be seen that the real domain sizes of the β phase formed from the pure elements result similar for both configurations and are smaller than for the milled alloy. This is probably an indication that the crystallite size of the β phase would depend on the starting material. The powders that result from the high configuration have a strain and a faulting probability higher than those from the low one. This latter result is consistent with the accumulation of strains for higher milling times.

It can also be seen in Table 1 that the strains are anisotropic. In order to analyze the behavior of the stresses, the strains were multiplied by the corresponding Young's moduli E(h k l) [14], which were calculated from the elastic constants [15]. The Young's moduli are 88.2 GPa for the 1 1 0 and 2 1 1 directions and 34.8 GPa for 2 0 0. The corresponding stresses are shown in Table 2, where their anisotropy becomes evident. Therefore, neither a constant stress nor a constant strain condition applies to the present material.

It has been found that when the pure elements of different crystal structures are milled in a high energy device, the final crystallite sizes scale well with the reciprocal of the melting temperature (T_m) [16]. In the present case, with a T_m of nearly 1150 K, a size of around 19 nm would be predicted. This value is consistent with the range of apparent crystallite sizes obtained when the stacking faults in the bcc structure are not taken into account.

For the low energy milling performed in the present work, the real domain sizes (Table 2) are around the hundreds of nanometers. On the other hand, the TEM results (Fig. 4) show that the milled samples exhibit particles with very small crystallites (∼5 nm). The difference in sizes between both experimental techniques is probably due to the TEM sample, whose preparation method would affect the validity of the sampling.

4.3. Stability of the β phase

Fig. 8 shows that a phase mixture of α, γ and ε annealed at 373 K transformed partially to the β phase. This is an interesting effect because the assessed equilibrium β phase field in the Cu–Zn diagram is not well defined below 520 K [1]. The present result indicates that the β field can be extended to lower temperatures. The combined action of ball milling and low temperature thermal treatment has provided the free energy and the path to synthesize β phase at temperatures as low as 370 K.

The fact that the evolution of the powders is detected on approaching 370 K, brings forward evidence that mechanical alloying is due to the high reactivity of the freshly formed metal surfaces, together with an appropriate mixing of the elements favored by the concomitant reduction of the crystallite sizes. The high local strains additionally help on lowering the activation barriers for atomic movements [4].

5. Conclusions

From the present results, the following conclusions can be drawn:

1- The β phase of Cu–Zn in stoichiometric composition is stable under low energy mechanical milling. No evidence of other crystalline or amorphous phases was obtained. The B2 order is retained during milling.
2- The evolution of the phases during low energy mechanical alloying of equal amounts of Cu and Zn atoms depend on the milling intensity.
3- Milling under an Ar atmosphere was found to be an effective way to avoid the oxide formation.
4- Special care has to be taken when analyzing the peak broadening from X-ray diffractograms of the β phase, due to the influence of the stacking faults on the shape of the characteristic peaks.
5- The temperature of the powder was found to remain below 370 K during the low energy ball milling.
6- Experimental evidence of the β phase stability at 370 K was found, suggesting that the β field of the Cu–Zn phase diagram can be extended to this range of low temperatures.

Acknowledgements

This work was supported by the ANPCyT, CONICET, CNEA and Universidad Nacional de Cuyo, Argentina.

References

[1] T. Massalski, H. Okamoto, P. Subramanian, L. Kacprzak (Eds.), Binary Alloy Phase Diagrams, second ed., American Society for Metals, Metals Park, Ohio, 1990.
[2] M. Ahlers, Prog. Mater. Sci. 30 (1986) 135–186.
[3] H.E. Troiani, A. Tolley, M. Ahlers, Philos. Mag. A 80 (2000) 1379–1391.
[4] C. Suryanarayana, Prog. Mater. Sci. 46 (2001) 1–184.
[5] J. Eckert, L. Schultz, E. Hellstern, K. Urban, J. Appl. Phys. 64 (1988) 3224–3228.
[6] S.K. Pabi, J. Joardar, B.S. Murty, J. Mater. Sci. 31 (1996) 3207–3211.
[7] B.T. McDermott, C.C. Koch, Scripta Metall. 20 (1986) 669–672.
[8] S. Martelli, G. Mazzone, S. Scaglione, M. Vittori, J. Less-Common Met. 145 (1988) 261–270.
[9] A. Calka, A.P. Radlinski, Mater. Sci. Eng. A134 (1991) 1350–1353.
[10] R.A. Young, A. Sakthivel, T.S. Moss, C.O. Paiva-Santos, J. Appl. Crystallogr. 28 (1995) 366–367.
[11] F. Delogu, L. Schiffini, G. Cocco, Philos. Mag. A 81 (2001) 1917–1937.
[12] J.I. Langford, R. Delhez, Th.H. de Keiser, E.J. Mittemeijer, Aust. J. Phys. 41 (1988) 173–187.
[13] B.E. Warren, X-Ray Diffraction, Dover Publications Inc., New York, 1990.
[14] D.E. Mikkola, J.B. Cohen, in: J.B. Cohen, J.E. Hilliard (Eds.), Local Atomic Arrangements studied by X-Ray Diffraction, Gordon and Breach, New York, 1966, p. 290.
[15] S. Shimizu, Y. Murakami, S. Kachi, J. Phys. Soc. Jpn. 41 (1976) 79–84.
[16] F. Delogu, G. Cocco, Mater. Sci. Eng. A 422 (2006) 198–204.